Progress In Electromagnetics Research M, Vol. 50, 1–10, 2016

Correlation Effects on the MIMO Capacity for Conformal Antennas on a Paraboloid

Christos Kalialakis[1, *], Theodoros N. Kaifas[2], and Apostolos Georgiadis[3]

Abstract—The use of conformal antennas in a MIMO link scenario is investigated. Conformal slot antennas are considered both in the transmitter and the receiver. First, a new modified correlation coefficient is derived that goes beyond the Clarke coefficient and takes into account the element radiation pattern. Secondly, a hybrid formulation that accounts for the impact of the mutual coupling and the pattern dependent correlation on the capacity is presented. The mutual coupling for slots placed circumferentially on a paraboloid substrate is derived using a rigorous approach based on Uniform Theory of Diffraction (UTD). The capacity is evaluated for the case of Rayleigh fading channel considering the new pattern dependent correlation coefficient and the conformal antenna mutual coupling. The planar case is included as a limiting case. It is shown that for conformal antennas on a paraboloid the capacity degradation compared to the planar case is up to 0.5 bps/Hz due to coupling and correlation.

1. INTRODUCTION

MIMO systems have drawn extensive interest as choices for high data rate wireless communications systems. Alternatively, MIMO can offer diversity that results in an increased link reliability. These advantages are possible by using multiple antennas both in the transmitter and the receiver while utilizing signal processing techniques [1]. A quality measure of a MIMO link is its capacity. Theoretically and under ideal conditions the capacity of the MIMO system increases with the number of antennas used [2]. However, this only holds when the signals are completely uncorrelated, a condition that is not true in the vast majority of practical situations [3–5]. The MIMO capacity (in bps/Hz) is evaluated in an average sense [6, 7], considering the fading nature of the wireless channels usually described by statistics.

Correlation has two constituents. The first correlation constituent is due to the effect of the mutual coupling of the antenna array elements which is independent of the incoming wave distribution. Mutual coupling is considered a complex problem that is dependent on the antenna type and the element positions in the array. Several previous works have shown the effect of mutual coupling on the system capacity for relatively simple antenna elements and only linear geometries. For example, in [8] the capacity of a MIMO system was evaluated in the case of dipoles. In [9] inverted-F antennas were considered in the system. In addition to coupling, the matching impact has been investigated in [10] using dipoles and in [11] using microstrip patches. In these cases, the coupling is evaluated with either equivalent circuit methods or measurements. Overall in order to properly determine the system capacity, it is necessary to know the mutual coupling between the antenna elements. For complicated antenna geometries such as conformal arrays full wave analysis and rigorous electromagnetic analysis is

Received 18 July 2016, Accepted 4 September 2016, Scheduled 12 September 2016

* Corresponding author: Christos Kalialakis (christos.kalialakis@cttc.es).

[1] Centre Tecnologic de Telecomunicacions de Catalunya-CTTC, Castelldefels 08860, Barcelona, Spain. [2] Radiocommunications Laboratory, Aristotle University of Thessaloniki, GR54124, Thessaloniki, Greece. [3] Institute of Sensors, Signals and Systems, School of Engineering and Physical Sciences, Heriot-Watt University, Edinburgh, Scotland, UK.

indispensable [12]. Conformal antenna arrays are utilized in airborne and space vehicles and also find applications in situations where surface adaptation is required (e.g., environmentally friendly cellular base stations) or flexible substrates [13–15]. Several conformal antennas have been suggested for MIMO use focusing only on mutual coupling but without any capacity calculations [16–20].

The second correlation constituent originates on the angular distribution of the waves that are being received. The distribution type is generally different in the case of a mobile terminal compared to a base station antenna. Several correlation models are used such as Clarke's model [21] for the terminal and the model known as Geometrically Based Simple Bounce (GBSB) [22] in the case of a base station. However, these models fail to account for the angular distributions of the antenna pattern because of the underlying assumption of 2D omnidirectional patterns. The breakdown of such assumption is especially prominent in the case of conformal antennas. In order to remedy this issue, full account of the conformal antenna element pattern is taken into consideration in this work for the first time.

In Section 2, slot antennas on a perfectly conducting paraboloid are introduced and the mutual coupling evaluation formulation is given based on an improved UTD and spectral domain approach [23]. In Section 3 the wave correlation coefficient that takes into account the angular distribution of the antenna element pattern is derived for the first time. Furthermore, in Section 4, the capacity formulation for multi-element antennas is introduced that utilizes the antenna array impedance matrix approach for the coupling [24] and the pattern dependent correlation. Results are presented in Section 5 for several link scenarios focusing on a 2×2 antenna configuration Different mutual coupling scenarios and correlation degrees among the slots are considered in order to determine the system performance in terms of its capacity. Conclusions are drawn in Section 6.

2. MUTUAL COUPLING OF SLOTS ON A PARABOLOID

A conformal multielement antenna geometry which consists of slots placed circumferentially on a paraboloid is utilized in this work. The geometry of this supporting structure and the position of the slots are shown in Figure 1(a).

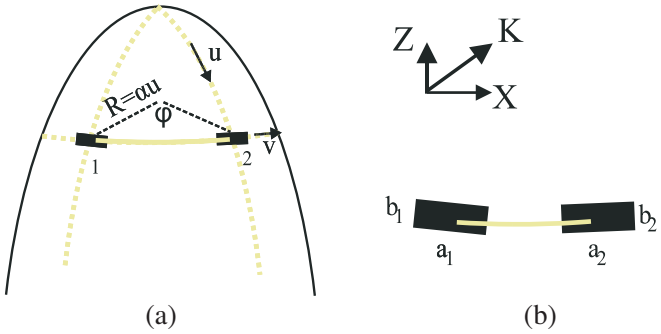

Figure 1. Geometry of conformal slot antennas, (a) antennas placed on the ring circumferentially on a perfectly conducting paraboloid along a ring of radius R and sharpness a, (b) dimension details of slot antennas.

Points on the paraboloid surface have coordinates u, v which obey the following parametric equations [25]:

$$x = au\cos v \quad y = au\sin v \quad z = -u^2 \tag{1}$$

where a is the sharpness/flatness parameter.

The rigorous method to evaluate the mutual coupling is adapted from [23, 25] and it is based on the Uniform Theory of Diffraction, [23, 26, 27] due to the curved conducting surface.

Consider two slots positioned on a conducting paraboloid with S being the geodesic distance (Figure 1). The first slot with dimensions $A_1 = a_1 b_1$ is placed at coordinates (u_1, v_1) while the second with dimensions $A_2 = a_2 b_2$ is placed at (u_2, v_2). Using the dominant magnetic current mode approximation (with $\bar{M}_u$ and $\bar{M}_v$ its $\bar{u}$ and $\vec{v}$ vector components) the mutual admittance Y_{12} is given

by [23]:

$$\begin{aligned} &-Y_{12}\cdot N_1\cdot N_2 \\ &= \iint\limits_{A_1}\iint\limits_{A_2}\left[\begin{array}{cc}\vec{M}_{u_1} & \vec{M}_{v_1}\end{array}\right]\left[\begin{array}{cc}\widehat{u}_1\cdot\widehat{t}_1 & \widehat{u}_1\cdot\widehat{b}_1\\ \widehat{v}_1\cdot\widehat{t}_1 & \widehat{v}_1\cdot\widehat{b}_1\end{array}\right]\left[\begin{array}{cc}T_{t_1t_2} & T_{t_1b_2}\\ T_{b_1t_2} & T_{b_1b_2}\end{array}\right]\left[\begin{array}{cc}\widehat{t}_2\cdot\widehat{u}_2 & \widehat{t}_2\cdot\widehat{v}_2\\ \widehat{b}_2\cdot\widehat{u}_2 & \widehat{b}_2\cdot\widehat{v}_2\end{array}\right]\left[\begin{array}{c}\vec{M}_{u_2}\\ \vec{M}_{v_2}\end{array}\right]dA_1dA_2 \end{aligned} \quad (2)$$

The unit vectors $\widehat{t}_1$ are tangent to the geodesic that connects the source with the detachment point that is related with the far field calculation. The b vectors are along the short dimension of each slot. The normalization constants N_1, N_2 are equal to

$$N_1=\sqrt{a_1b_1/2},\quad N_2=\sqrt{a_2b_2/2} \quad (3)$$

and the T coefficients are given in [26]. The off-diagonal elements of the T matrix are much smaller than the diagonal ones i.e.,

$$|T_{bt}|\ll|T_{tt}|,\quad |T_{bt}|\ll|T_{bb}| \quad (4)$$

For circumferential slots i.e., along vector $\vec{v}$, the magnetic current mode component

$$\vec{M}_u=\vec{0} \quad (5)$$

and taking into account Equation (5), mutual admittance in Equation (2) becomes:

$$\begin{aligned} &Y_{12}\cdot N_1\cdot N_2 \\ &= -\iint\limits_{A_1}\iint\limits_{A_2}M_{v_1}\left[\left(\widehat{v}_1\cdot\widehat{t}_1\right)T_{t_1t_2}\left(\widehat{t}_2\cdot\widehat{v}_2\right)+\left(\widehat{v}_1\cdot\widehat{b}_1\right)T_{b_1b_2}\left(\widehat{b}_2\cdot\widehat{v}_2\right)\right]M_{v_2}dA_1dA_2 \end{aligned} \quad (6)$$

A compact notation for the internal vector products in Eq. (6) is introduced,

$$\begin{aligned} s_1&=\left(\widehat{v}_1\cdot\widehat{t}_1\right)\quad c_1=\left(\widehat{v}_1\cdot\widehat{b}_1\right)\\ s_2&=\left(\widehat{t}_2\cdot\widehat{v}_2\right)\quad c_2=\left(\widehat{b}_2\cdot\widehat{v}_2\right)\end{aligned} \quad (7)$$

Expression (6) is transformed via Equation (7) as follows

$$Y_{12}\cdot N_1\cdot N_2=-\iint\limits_{A_1}\iint\limits_{A_2}M_{v_1}\left[\left(s_1s_2\right)T_{t_1t_2}+\left(c_1c_2\right)T_{b_1b_2}\right]M_{v_2}dA_1dA_2 \quad (8)$$

Equation (8) is used for the calculation of the results in Section 5. The mutual admittance for the planar slots is given by the same expression but with T coefficients that take asymptotically the form [23]

$$\begin{aligned} T_{tt}&\to G_0+G_1\\ T_{bb}&\to G_1\end{aligned} \quad (9)$$

where

$$\begin{aligned} G_0&=\left[\frac{-1-jk_oS+k_o^2S^2}{S^3}\right];\quad k_o=2\pi/\lambda_o\\ G_1&=\left[\frac{3+3jk_oS-k_o^2S^2}{S^3}\right]\end{aligned} \quad (10)$$

In case the slots are nearly parallel the T_{bb} term dominates, whereas when the slots are collinear, the T_{tt} term dominates.

3. CORRELATION FORMULATION

3.1. Correlation: General Case

The correlation coefficient between two antenna elements, without mutual coupling, is defined by, [24, Eq. (19.67)]:

$$\rho_{12}^{OC}=\frac{\left\langle V_1^{OC}\cdot\left(V_2^{OC}\right)^*\right\rangle}{\sqrt{\left\langle\left|V_1^{OC}\right|^2\right\rangle\left\langle\left|V_2^{OC}\right|^2\right\rangle}} \quad (11)$$

where V_v^{OC}, the open circuit voltage induced in the v-th receiving element. V_v^{OC} is also the v-th element of the $\mathbf{V}^{OC}$ column vector:

$$\mathbf{V}^{OC} = \left[\; F_1\left(\theta,\phi\right)\exp\left(-j\bar{k}\bar{r_1}\right) \quad F_v\left(\theta,\phi\right)\exp\left(-j\bar{k}\bar{r_v}\right) \quad F_N\left(\theta,\phi\right)\exp\left(-j\bar{k}\bar{r_N}\right) \; \right]^T \tag{12}$$

In Equation (12), $F_v(\theta,\phi)$ is the element field pattern given by:

$$F_v(\theta,\phi) = \mathbf{h}_v \cdot \mathbf{E}_{inc} \tag{13}$$

$\mathbf{h}_v$ is the vector effective length of the v-th element. $\vec{r}_v$ is the position vector of the v-th element of the array. $\mathbf{E}_{inc}$ is the incident plane wave.

Due to Equations (12) and (13), Equation (11) takes the form:

$$\rho_{12}^{OC} = \frac{\left\langle F_1\left(\theta,\phi\right)F_2^*\left(\theta,\phi\right)\exp\left[-j\bar{k}\left(\bar{r_1}-\bar{r_2}\right)\right]\right\rangle}{\sqrt{\left\langle F_1\left(\theta,\phi\right)F_1^*\left(\theta,\phi\right)\right\rangle\left\langle F_2\left(\theta,\phi\right)F_2^*\left(\theta,\phi\right)\right\rangle}} \tag{14}$$

Equation (14) is the general expression for the correlation coefficient that takes into account the use of directive radiators. Therefore, the most accurate correlation representation is possible when using Equation (14).

3.2. Correlation: Circumferential Slots on a Paraboloid

Expression (14) is quite general. In this section, the correlation is found for the specific geometry of slots placed on a paraboloid. For the horizontal plane where $\theta = \pi/2$, Equation (14) is transformed to

$$\rho_{12}^{OC} = \frac{\left\langle F_1\left(\pi/2,\phi\right)F_2^*\left(\pi/2,\phi\right)\exp\left[-j\bar{k}\left(\bar{r_1}-\bar{r_2}\right)\right]\right\rangle}{\sqrt{\left\langle F_1\left(\pi/2,\phi\right)F_1^*\left(\pi/2,\varphi\right)\right\rangle\left\langle F_2\left(\pi/2,\phi\right)F_2^*\left(\pi/2,\phi\right)\right\rangle}} \tag{15}$$

Taking into account that the following conditions hold, a) rotational symmetry b) same type elements and c) the elements are arranged in a ring of radius R, then the element pattern obeys:

$$F_v\left(\pi/2,\phi\right) = F\left(\pi/2,\phi-\phi_v\right) \tag{16}$$

where ϕ_v is the azimuth angle of the v-th element.

The actual form of the element pattern can result from theory or radiation pattern measurements. For the case under study i.e., circumferential paraboloidal slots, the element pattern can be approximated by [23, 32]:

$$F\left(\pi/2,\phi\right) = \left(\frac{1+\cos\phi}{2}\right)^b \tag{17}$$

where b is the directivity exponent.

The nominator of the correlation coefficient in Equation (14) using Equations (6) and (7) is calculated as follows,

$$\begin{aligned} &\left\langle F_1\left(\pi/2,\phi\right)F_2^*\left(\pi/2,\phi\right)\exp\left[-j\bar{k}\left(\bar{r_1}-\bar{r_2}\right)\right]\right\rangle \\ &= \int_0^{2\pi} d\phi f(\phi)\left(\frac{1+\cos\left(\phi-\phi_1\right)}{2}\right)^b\left(\frac{1+\cos\left(\phi-\phi_2\right)}{2}\right)^b\exp\left[-j\bar{k}\left(\bar{r_1}-\bar{r_2}\right)\right] \end{aligned} \tag{18}$$

The following expressions are introduced to facilitate computation of Equation (18),

$$\Delta\vec{r} = \vec{k}\left(\vec{r}_1-\vec{r}_2\right) \tag{19}$$

$$\vec{r}_{1,2} = R\cdot\left(\cos\phi_{1,2}\widehat{x}+\sin\phi_{1,2}\widehat{y}\right) \tag{20}$$

$$\vec{k} = -k\left(\cos\phi\widehat{x}+\sin\phi\widehat{y}\right) \tag{21}$$

The argument of the exponential term in Equation (18), utilizing Equations (20) and (21), is now written as

$$\Delta\vec{r} = k\left(\cos\phi\widehat{x}+\sin\phi\widehat{y}\right)\left[R_1\left(\cos\phi_{1,2}\widehat{x}+R_1\sin\phi_{1,2}\widehat{y}+\widehat{z}_1\right)\right]\left[R_2\left(\cos\phi_{1,2}\widehat{x}+R_2\sin\phi_{1,2}\widehat{y}+\widehat{z}_2\right)\right] \tag{22}$$

Since the slots are placed on a ring then due to rotational symmetry,

$$\phi_1 = -\phi_2 = \bar{\phi} \tag{23}$$

The argument of the exponential term in Equation (22) can now be written as

$$\Delta\vec{r} = \left[-k\left(\widehat{x}\cos\phi + \widehat{y}\sin\phi\right)\right]\left[\left(\widehat{x}R_1(\cos\bar{\phi} + \widehat{y}\sin\bar{\phi}\right) - \left(R_2(\cos\bar{\phi}\widehat{x} - \sin\bar{\phi}\widehat{y})\right)\right] \tag{24}$$

Following some algebra, Equation (24) can be expressed as

$$\Delta\vec{r} = -k\left(\widehat{x}\cos\phi + \widehat{y}\sin\phi\right)\left(\Delta R\cos\bar{\phi}\widehat{x} + \Sigma R\sin\bar{\phi}\widehat{y}\right) \tag{25}$$

Or equivalently

$$\Delta\vec{r} = -k\left(\Delta R\cos\bar{\phi}\cos\phi\widehat{x} + \Sigma R\sin\bar{\phi}\sin\phi\widehat{y}\right) \tag{26}$$

where

$$\Delta R = R_1 - R_2$$
$$\Sigma R = R_1 + R_2$$

Assuming further that $f(\phi) = 1$ and using Equations (26) and (29) the nominator of the correlation coefficient is now expressed as

$$\begin{aligned}&\left\langle F_1\left(\pi/2,\phi\right)F_2^*\left(\pi/2,\phi\right)\exp\left[-j\bar{k}\left(\bar{r_1} - \bar{r_2}\right)\right]\right\rangle \\ &= \int_0^{2\pi} d\phi\left(\frac{1+\cos\left(\phi-\bar{\phi}\right)}{2}\right)^b\left(\frac{1+\cos\left(\phi+\bar{\phi}\right)}{2}\right)^b\exp\left[jk\left(\Delta R\cos\bar{\phi}\cos\phi + \Sigma R\sin\phi\sin\phi\right)\right]\end{aligned} \tag{27}$$

Correspondingly, the denominator of the correlation coefficient is given by

$$\left\langle F_1\left(\pi/2,\phi\right)F_1^*\left(\pi/2,\phi\right)\right\rangle = \left\langle F_2\left(\pi/2,\phi\right)F_2^*\left(\pi/2,\phi\right)\right\rangle = \int_0^{2\pi} d\phi\left(\frac{1+\cos\phi}{2}\right)^{2b} \tag{28}$$

Usually expressions such as Equations (27) and (28) can be computed numerically. Apart from numerical quadrature, a closed form evaluation is feasible in certain cases. For the case under consideration i.e., slots on a ring and for a directivity exponent $b = 1$, the closed form is derived in this work for the first time as;

$$\rho = \frac{2}{3}J_0(A)\left[1 + \frac{1}{2}\cos 2\bar{\varphi}\right] + j\frac{4}{3}J_1(A)\cos\bar{\varphi}\cos\xi - \frac{1}{3}J_2(A)\cos 2\xi \tag{29}$$

where $J_n(A)$ is the Bessel function of the first kind and

$$A = k\sqrt{\Delta R^2\cos^2(\bar{\phi}) + \Sigma R^2\sin^2(\bar{\phi})} \tag{30}$$

$$\xi = \tan^{-1}\left(\frac{\Sigma R}{\Delta R}\tan\bar{\phi}\right) \tag{31}$$

Expression (29) is derived after some lengthy but standard analytical definite integral evaluations which originate from expanding Equations (27) and (28) into sums of integrals.

4. MIMO CAPACITY EVALUATION MODEL

Consider a wireless link utilizing M_{TX} antennas at the transmitter, M_{RX} antennas at the receiver. The link capacity C in bps/Hz [2] of the channel operating under a Signal-to-Noise Ratio SNR, is given by:

$$C = \log_2\left[\det\left(I_{M_R} + \frac{SNR}{M_T}\cdot H\cdot H'\right)\right] \tag{32}$$

where $I_{M_{RX}}$ is the identity matrix of order M_{RX}, H the system matrix, and the prime $'$ indicates the conjugate transpose of a matrix.

When a Kronecker channel model is used [28] the system matrix H is separable in transmitter and receiver matrices. Furthermore the model is valid for 2×2 MIMO that is used in this work and the model is useful for NLOS situations that can be modeled by Rayleigh fading. The capacity for such a model in a Rayleigh fading scenario reads [8, 11]:

$$C = \log_2 \left[\det \left(I_{M_R} + \frac{SNR}{M_T} \frac{1}{C_T^2} \frac{1}{C_R^2} K_R H_g K_T H_g^{'} \right) \right] \tag{33}$$

where H_g is a random complex Gaussian process that models a Rayleigh fading channel. The auxiliary quantities $K_T,\ C_T$, C_R, K_R are given by

$$K_R = Z_R(d_R)\rho_{12}(d_R)Z_R^{'}(d_R) \tag{34}$$

$$K_T = Z_T(d_T)\rho_{12}(d_T)Z_T^{'}(d_T) \tag{35}$$

$$C_R = \frac{Z_{11}^{R*}}{Z_{11}^{R} + Z_{11}^{R*}} \tag{36}$$

$$C_T = \frac{Z_{11}^{T*}}{Z_{11}^{T} + Z_{11}^{T*}} \tag{37}$$

where d_T and d_R are the distances between the elements in the transmitter and in the receiver arrays respectively, $\rho_{12}(d_R)$ and $\rho_{12}(d_T)$ are the correlation coefficients between the antennas at the transmitter and receiver. Z_R and Z_T relate the impedance matrices Z^T and Z^R with the source and the load impedances Z_S and Z_L. The source impedance is located at the transmitter and the load impedance is located at the receiver. A reference impedance $Z_{\mathrm{O}} = 50\,\Omega$ is assumed. Conjugate matching of source and load to the antenna elements is assumed. Equivalently admittances or S-parameters can be used which can then be transformed to impedances via standard formulas [29].

The impedance matrix can be evaluated via computational methods or analytically using rigorous electromagnetic analysis such as the UTD approach in the Section 2 [23, 25]. The matrix can be also filled by using experimental data usually in the form of S-parameters [30].

5. RESULTS

5.1. Evaluation of Mutual Coupling

In this section, results are presented for the mutual coupling between two slots positioned circumferentially (E-plane) on a perfectly conducting paraboloid. The slot dimensions are $\lambda/2 \times \lambda/5$ and the sharpness parameter a is set equal to 1/2. For all computations using the azimuth angle, φ, as a parameter, the position of the first slot is considered fixed at $(u_1 = 2, v_1 = -\pi/2)$. The second slot is moving on the path $u_2 \in (1, 3)$ and $v_2 = v_1 + \phi$. For a set of given coordinates, a decreased value of parameter α brings the slot closer and the coupling gets stronger.

In Figure 2 the mutual impedance between two slots on the paraboloid is shown for two different values of the azimuth angle φ. Each slot is fed by a rectangular waveguide in the dominant vector mode.

5.2. The Pattern Dependent Correlation

The slot pattern dependent correlation has been evaluated both numerically using Equations (27) and (28) and by the closed form in Equation (29) as a function of φ (Figure 3). The numerical integration is done via a Legendre-Gauss quadrature. The required quadrature computations were performed using the open source Matlab function lgwt.m [31]. Excellent agreement is observed between numerical integration and the closed form in Equation (29).

5.3. Capacity under Mutual Coupling and a Pattern Dependent Correlation

A 2×2 MIMO link is assumed using slots on paraboloids for both the transmitter and receiver side. The transmitter has two elements of a fixed size $\lambda/2 \times \lambda/5$ separated by 0.35λ for the frequency of interest.

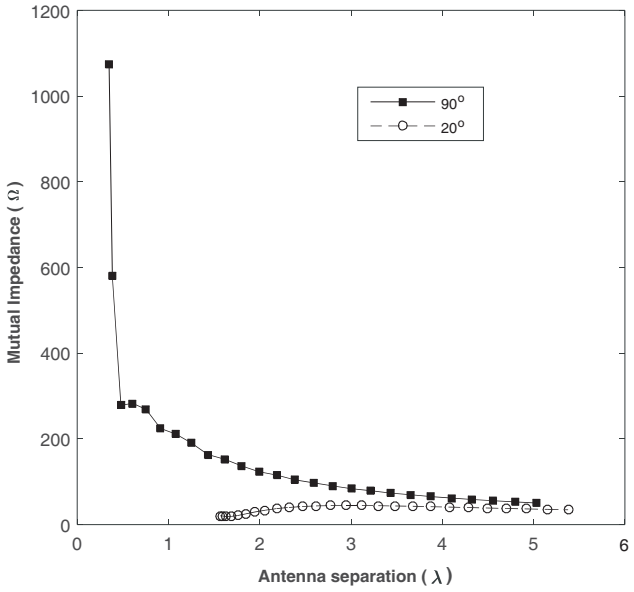

Figure 2. Mutual coupling in terms of impedance as a function of the slot separation (sharpness parameter $\alpha = 1/2$) with the azimuth φ taking values 20 and 90 degrees.

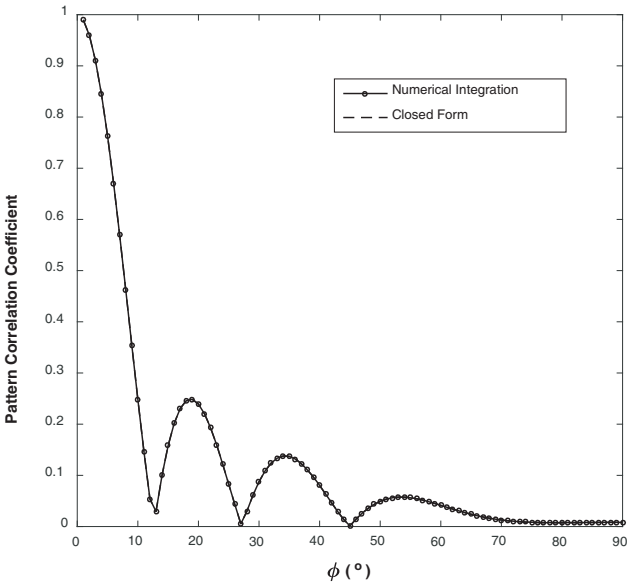

Figure 3. The correlation coefficient for the case of two circumferential slots on a paraboloid as a function of φ in the case of $(u_1, u_2) = (2, 2)$.

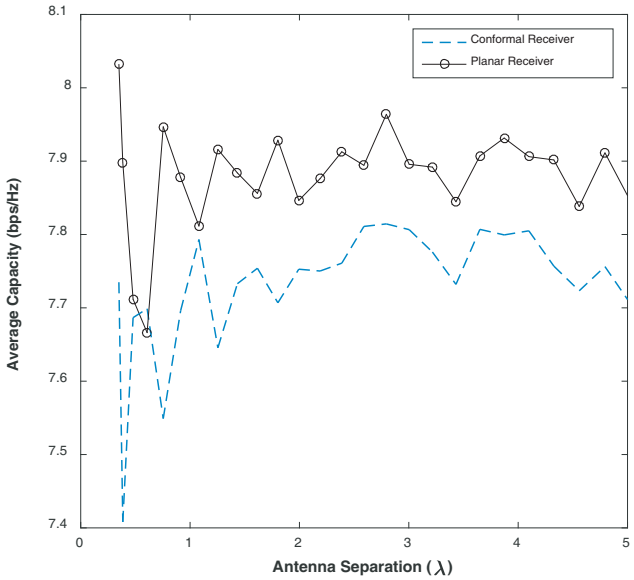

Figure 4. Average capacity of a 2×2 MIMO link as a function of the slot distance separation at the receiver ($\varphi = 20°$, $SNR = 10\,\text{dB}$, 3000 samples of the complex Gaussian process). The transmitter is considered conformal.

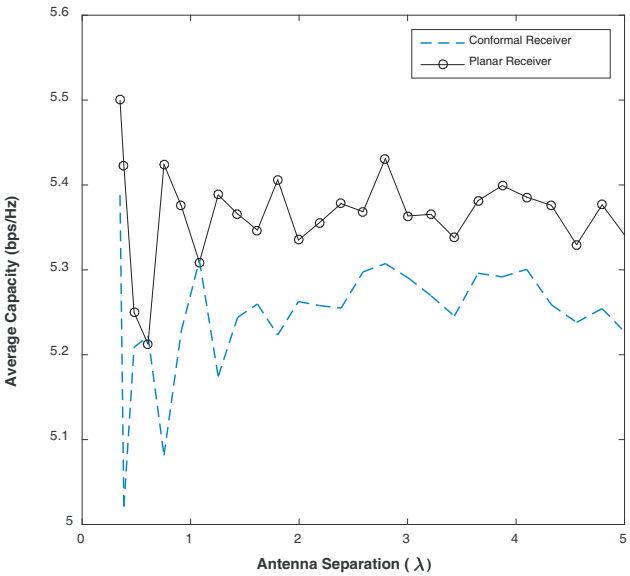

Figure 5. Average capacity of 2×2 MIMO Link as a function of the slot distance separation at the receiver ($\varphi = 20°$, $SNR = 10\,\text{dB}$, 3000 samples of the Gaussian process). The transmitter is considered planar.

In case of a wideband signal transmission, the computation must be repeated for the corresponding bandwidth. The capacity is calculated as function of the receiver element separation.

A Rayleigh fading channel is realized using random samples of a complex Gaussian process. Each displayed capacity value in Figure 4 is an average over 3000 channel realizations and corresponding

capacity samples. Ideal matching is assumed.

In Figure 4 the capacity is evaluated for different values of the azimuth parameter φ between the receiver elements calculated as a function of the separation between the two slots whereas φ is fixed for the transmitter. The planar case has also been evaluated. The transmitter is considered to be a pair of conformal slots with a fixed φ separation.

In Figure 5 the capacity is evaluated for both planar and conformal receiver configurations but with the transmitter now being a planar slot array.

It can be observed that the mutual coupling at the receiver has an impact on the capacity which is more evident for small antenna separations. As the separation gets larger the coupling becomes less pronounced and the variations are more due to pattern correlation.

The physical basis for the capacity degradation of the conformal case is the pattern dependent correlation. In other words, due to the curvature and their different orientation the conformal antenna elements do not face the incoming waves with the same phase. In the planar case, the antennas are in a much larger degree exposed to the incoming waves in a similar way.

Overall the use of conformal geometry tends to lower the mean capacity, a fact to be taken into account when using such arrays for a MIMO link.

6. CONCLUSIONS

In this work, a rigorous approach has been presented that take account for the wave correlation model and the mutual coupling effect when a conformal antenna is used. A modified wave correlation coefficient which takes into account the antenna element radiation pattern has been presented in the case of slots on a paraboloid. A closed form was derived for the case of slots placed on a ring and compared favourably with a numerical solution. The impact of the correlation on the capacity of a MIMO system has been studied. The obtained results have shown how the capacity of the system is affected when the slots are conformal. In the 2×2 case the capacity degrades by up to 0.5 bps/Hz and should be taken into account when using such antennas. The hybrid method in this work can be extended to other propagation models and other curved surfaces that support conformal geometries in order to evaluate accurately any performance degradation due to coupling or correlation when MIMO operation is required.

ACKNOWLEDGMENT

The work of Christos Kalialakis and Apostolos Georgiadis has been supported by European Union's Horizon 2020 research and innovation programme under the Marie Sklodowska-Curie grant agreement No 654734. The work of A. Georgiadis was also supported by EU H2020 Marie Sklodowska-Curie Grant Agreement 661621. The authors acknowledge EU COST Action IC1301 Wireless Power Transmission for Sustainable Electronics.

REFERENCES

1. Gesbert, D., M. Shafi, D.-S. Shiu, et al., "From theory to practice: An overview of space time coded wireless systems," *IEEE Journal on Selected Areas in Communications*, Vol. 21, 283–302, 2003.
2. Foschini, G. J. and M. J. Gans, "On limits of wireless communications in a fading environment when using multiple antennas," *Wireless Personal Communications*, Vol. 6, No. 3, 311–335, Mar. 1998.
3. Shiu, D. S., J. Foschini, J. Gans, and J. M. Kahn, "Fading correlation and its effect on the capacity of multielement antenna system," *IEEE Transactions on Communications*, Vol. 48, 502, 2000.
4. Clerckx, B. and C. Oestges, *MIMO Wireless Networks: Channels, Techniques and Standards for Multi-antenna, Multi-user and Multi-cell Systems*, Academic Press, 2013.
5. Nyberg, D., P. S. Kildal, A. Gummalla, and J. Carlsson, "Degradation of MIMO capacity due to correlation and efficiency of practical antennas," *International Symposium on Antennas and Propagation*, Taipei, Taiwan, Oct. 27–30, 2008.

6. Gesbert, D,, H. Bolcskei, D. Gore, and A. Paulraj, "MIMO wireless channels: Capacity and performance prediction," *IEEE Global Telecommunications Conference (GLOBECOM'00)*, Vol. 2, 2000.
7. Varzakas, P., "Average channel capacity for rayleigh fading spread spectrum MIMO systems," *International Journal of Communication Systems*, Vol. 19, No. 10, 1081–1087, Dec. 2006.
8. Janaswamy, R., "Effect of mutual coupling on the capacity of fixed length linear arrays," *IEEE Antenna and Wireless Propagation Letters*, Vol. 1, 157–160, 2002.
9. Chae, S., S. Oh, and S. Park, "Analysis of mutual coupling, correlations, and TARC in WiBro MIMO array antenna," *IEEE Antennas and Wireless Propagation Letters*, Vol. 6, 122–125, 2007.
10. Fei, Y., Y. Fan, B. K. Lau, and J. S. Thompson, "Optimal single-port matching impedance for MIMO capacity maximization," *IEEE Transactions on Antennas and Propagation*, Vol. 56, No. 11, 3566–3575, Nov. 2008.
11. Kalialakis, C., A. Collado, and A. Georgiadis, "Capacity of linear rectangular microstrip antenna arrays," *Proceedings of 3rd European Conference on Antennas and Propagation (EuCAP 2009)*, Berlin, Germany, Mar. 23–27, 2009.
12. Josefsson, L. and P. Persson, *Conformal Array Antenna Theory and Design*, John Wiley & Sons, 2006.
13. Adams, J. J., E. B. Duoss, T F. Malkowski, et al., "Conformal printing of electrically small antennas on three-dimensional surfaces," *Advanced Materials*, Vol. 23, No. 11, 1335–1340, Mar. 18, 2011.
14. Nikolaou, S., G. E. Ponchak, J. Papapolymerou, and M. M. Tentzeris, "Conformal double exponentially tapered slot antenna (DETSA) on LCP for UWB applications," *IEEE Transactions on Antennas and Propagation*, Vol. 54, No. 6, 1663–1669, 2006.
15. Boeykens, F., L. Vallozzi, and H. Rogier, "Cylindrical bending of deformable textile rectangular patch antennas," *International Journal on Antennas and Propagation*, Article ID 17020, 11 pages, 2012.
16. Tunc, C., A. E. Irci, O. Bakir, et al., "Investigation of planar and conformal printed arrays for MIMO performance analysis," *European Conference on Antennas and Propagation (EuCAP)*, 1–6, Nov. 6–10, 2006.
17. Craddock, I. J., D. L. Paul, C. M. Tan, et al., "Investigation of array performance for MIMO channel characterisation," *URSI EMTheory Symposium*, 69–71, 2004.
18. Orlob, C., Q. H. Dao, and B. Geck, "Conformal log-periodic antenna with integrated feeding network for UWB-MIMO applications," *7th German Microwave Conference (GeMiC)*, 1–4, Mar. 12–14, 2012.
19. Yetisir, E., D. Psychoudakis, and J. L. Volakis, "Small size conformal UWB arrays for MIMO and diversity applications," *IEEE Antennas and Propagation Society International Symposium*, Jul. 8–14, 2012.
20. Gamage, J. K. H., B. Holter, J. A. Jensen, et al., "A wideband conformal antenna array for cognitive radio/MIMO applications," *European Conference on Antennas and Propagation (EUCAP)*, 725–729, Apr. 11–15, 2011.
21. Clarke, R. H., "A statistical theory of mobile radio reception," *Bell Systems Technical Journal*, Vol. 47, No. 6, 957–1000, Jul.–Aug. 1968.
22. Petrus, P., J. Reed, and T. S. Rappaport, "Geometrical-based statistical macrocell channel model for mobile environments," *IEEE Transactions on Communications*, Vol. 50, 495–502, 2002.
23. Kaifas, T. N., T. Samaras, K. Siakavara, and J. N. Sahalos, "A UTD-OM technique to design slot arrays on a perfectly conducting paraboloid," *IEEE Transactions on Antennas and Propagation*, Vol. 53, No. 5, 1688–1698, May 2005.
24. Janaswamy, R., "Spatial diversity for wireless communication systems," *Handbook of Antennas in Wireless Communications*, Chap. 19, L. C. Godara, ed., CRC Press, 2002.
25. Lipschutz, M. M., *Differential Geometry*, McGraw-Hill, New York, 1995.
26. Pathak, P. and N. Wang, "Ray analysis of mutual coupling between antennas on a convex surface," *IEEE Trans. Antennas Propagat.*, Vol. 29, No. 6, 911–922, 1981.

27. Pathak, P., N. Wang, W. D. Burnside, and R. Kouyoumjian, "A uniform GTD solution for the radiation from sources on a convex surface," *IEEE Trans. Antennas Propagat.*, Vol. 29, No. 4, 609–622, 1981.
28. Wu, K. and B. Ottersten, "Models for MIMO propagation channels — A review," *Wirel. Commun. Mob. Comput.*, 653–666, 2002.
29. Pozar, D., *Microwave Engineering*, Addison-Wesley, 1993.
30. Kalialakis, C., D. Anagnostou, and M. Chryssomallis, "Mutual coupling effects on the MIMO capacity using dual band Wi-Fi double-T printed antennas," *2015 IEEE AP-S Symposium on Antennas and Propagation*, Vancoover, Canada, Jul. 2015.
31. Von Winckel, G., "Legendre-Gauss quadrature weights and nodes," authored 25/2/2004, Available at http://www.mathworks.com/matlabcentral/fileexchange/4540-legendre-gauss-quadrature-weights-and-nodes/content/lgwt.m.
32. Kaifas, T. N., "Study of systems of conformal arrays," PhD. Dissertation (in Greek), Dept. of Physics, Aristotle University of Thessaloniki, Greece, 2003.